Anisotropy of $Ca_{0.73}La_{0.27}(Fe_{0.96}Co_{0.04})As_2$ studied by torque magnetometry*

Ya-Lei Huang(黄亚磊)[1,2], Run Yang(杨润)[3], Pei-Gang Li(李培刚)[1,4,†], and Hong Xiao(肖宏)[2,‡]

[1] *Department of Physics, Zhejiang Sci-Tech University, Hangzhou* 310018, *China*
[2] *Center for High Pressure Science and Technology Advanced Research, Beijing* 100094, *China*
[3] *Laboratorium für Festkörperphysik, ETH–Zürich*, 8093, *Zürich, Switzerland*
[4] *Department of Physics, Beijing University of Posts and Telecommunications, Beijing* 100876, *China*

(Received 6 June 2020; revised manuscript received 12 June 2020; accepted manuscript online 23 June 2020)

Torque measurements were performed on single crystal samples of $Ca_{0.73}La_{0.27}(Fe_{0.96}Co_{0.04})As_2$ in both the normal and superconducting states. Contributions to the torque signal from the paramagnetism and the vortex lattice were identified. The superconducting anisotropy parameter γ was determined from the reversible part of the vortex contribution based on Kogan's model. It is found that $\gamma \simeq 7.5$ at $t = T/T_c = 0.85$, which is smaller than the result of $CaFe_{0.88}Co_{0.12}AsF$ $\gamma \simeq 15$ at $t = 0.83$, but larger than the result of 11 and 122 families, where γ stays in the range of 2–3. The moderate anisotropy of this 112 iron-based superconductor fills the gap between 11, 122 families and 1111 families. In addition, we found that the γ shows a temperature dependent behavior, i.e., decreasing with increasing temperature. The fact that γ is not a constant point towards a multiband scenario in this compound.

Keywords: torque, anisotropy parameter, superconductivity

PACS: 74.25.Ha, 74.25.Op, 74.70.Xa **DOI:** 10.1088/1674-1056/ab9f26

1. Introduction

Iron-based superconductors (FeSCs) include several families, such as 1111 family,[1–3] 122 family,[4] 111 family,[5] and 112 family.[6] Among them, $Ca_{1-x}La_xFeAs_2$ (CaLa112) is the first example of FeSCs which crystallizes in a monoclinic lattice with the space group of $P21$ (No. 4).[6] The presence of one-dimensional zig-zag As chains is the most prominent feature of the metallic block layer between the FeAs layers. Such metallic layers make the structure and electronic of CaLa112 distinct from other FeSCs. The temperature-doping phase diagram of CaLa112 is in stark contrast to many existing FeSCs, since the Neel temperature T_N of CaLa112 is found to increase with increasing x ($0.15 < x < 0.25$).[7] Intriguingly, T_N is gradually suppressed with electron doping (Co, Ni, or Pd substitution on the Fe site) and another superconducting phase is resolved.[8–10] The metallic spacer layers and the interesting phase diagram make CaLa112 particularly interesting.

The superconducting anisotropy parameter γ is an important quantity for characterizing superconductivity. From the standard anisotropic Ginzburg–Landau theory, $\gamma \equiv \sqrt{m_c^*/m_a^*} = H_{c2}^{||ab}/H_{c2}^{||c} = \lambda_c/\lambda_{ab} = \xi_{ab}/\xi_c$, where m is the effective mass, c and a are crystallographic axes, respectively, H_{c2} is the upper critical field, λ is the penetration depth, and ξ is the coherence length. For CaLa112 system, the anisotropy parameter γ is reported in a very limited temperature range close to T_c. For example, in $Ca_{0.82}La_{0.18}FeAs_2$, γ is 2–4 at $0.90 < t(T/T_c) < 0.96$.[11] For $Ca_{0.8}La_{0.2}Fe_{0.98}Co_{0.02}As_2$, γ is 2–6 at $0.95 < t < 0.98$.[12] In addition, the γ reported is based on transport measurement which is not a thermodynamic approach. Among many different techniques, torque magnetometry is the most sensitive one to detect anisotropy parameter especially with small single crystals.[13,14] Torque is a thermodynamic approach, which is defined by the angular derivative of the free energy.[15] It has been successfully applied to investigate the anisotropy of FeSCs, cuprates, heavy fermion superconductors,and intermetallic compounds, see our previous work[16–19] and other reports.[20–23]

$Ca_{0.73}La_{0.27}FeAs_2$ is regarded as a parent compound of 112 type iron-based superconductors. With Co substitution on Fe site, superconductivity is induced in the system. Here, we performed torque measurements on single crystal samples of $Ca_{0.73}La_{0.27}(Fe_{0.96}Co_{0.04})As_2$. Based on Kogan's model,[15] we obtained the anisotropy parameter γ and estimated the in-plane penetration depth λ_{ab}, an important characteristic length scale of a superconductor, which parameterizes the ability of a superconductor to screen an applied field by the diamagnetic response of the superconducting condensate. It was found that at the reduced temperature $t = 0.85$, $\gamma \simeq 7.5$. Thus, this material is more anisotropic compared to 11 and 122 families of FeSCs, whose γ is about 2–3.[24] It was found that γ is not constant, instead, it shows an obvious temperature dependence,

*Project supported by NSAF, China (Grant No. U1530402). P. G. Li acknowledges the support of the National Natural Science Foundation of China (Grant No. 51572241).

†Corresponding author. E-mail: pgli@bupt.edu.cn
‡Corresponding author. E-mail: hong.xiao@hpstar.ac.cn

which suggests a multiband picture.[25]

2. Methods

High quality single crystal samples of $Ca_{0.73}La_{0.27}(Fe_{0.96}Co_{0.04})As_2$ were grown by the self-flux method.[26] Electrical resistance measurements were performed in a physical property measurement system (PPMS). Magnetization measurements were performed by using a superconducting quantum interference device (SQUID). The sample for which the torque data is shown in this paper has a mass of 0.40 mg. Angular dependent torque measurements were performed by using a piezoresistive torque magnetometer in the PPMS. The angle θ is defined as the angle between the magnetic field and the c-axis of the single crystal. In this technique, a piezoresistor measures the torsion, or twisting, of the torque lever about its symmetry axis as a result of the magnetic moment of the sample. Note that the torque due to gravity and puck should always be subtracted from the total measured torque signal.[19]

3. Results and discussion

Figure 1(a) shows the temperature T dependent resistance R. The onset of the superconducting transition appears at $T_c^{\rm onset} = 20.0$ K and the zero resistance is reached at $T_{c0} = 17.5$ K. The magnetization M curves were measured under field-cooled (FC) and zero-field- cooled (ZFC) conditions with a magnetic field H of 10 Oe applied along the ab-plane of the crystal, as shown in Fig. 1(b). T_c^m determined from the magnetization measurements is 17.9 K, which is consistent with the T_{c0} obtained from the resistance measurements.

Figure 2(a) shows selected torque data measured in the normal state. It is found that torque τ is sinusoidal and can be well fitted by

$$\tau(T,H,\theta) = \tau_0(T,H)\sin 2\theta, \tag{1}$$

where τ_0 is a temperature and magnetic field dependent fitting parameter. Note that τ_0/H has a magnetic field H dependence at $T = 25$ K and 300 K as shown in Fig. 2(b). The solid lines are linear fits to the data, which show that τ_0/H is proportional to H, i.e.,

$$\tau_0(T,H) = A(T)H^2, \tag{2}$$

where A is a temperature dependent fitting parameter. Thus, the torque can be written by

$$\tau(T,H,\theta) = \tau_0 \sin 2\theta = A(T)H^2 \sin 2\theta. \tag{3}$$

From Eq. (3), the torque τ has a H^2 magnetic field dependence and $\sin 2\theta$ angular dependence. These two features are typical behaviors for paramagnetic response,[21]

$$\tau_p = \frac{\chi_c - \chi_{ab}}{2} H^2 \sin 2\theta, \tag{4}$$

where χ_{ab} and χ_c are the susceptibilities along ab-plane and c-axis of the single crystal, respectively. In FeSCs, χ_{ab} is bigger than χ_c, so τ_0 is negative.[16] It is different from heavy fermion superconductor $CeCoIn_5$ and cuprate superconductor $Tl_2Ba_2CuO_{6+\delta}$ where $\chi_c > \chi_{ab}$.[19,22] The paramagnetic behavior observed in $Ca_{0.73}La_{0.27}(Fe_{0.96}Co_{0.04})As_2$ is also reported in other FeSCs, such as $CaFe_{0.88}Co_{0.12}AsF$[16] and $LaFeAsO_{0.9}F_{0.1}$.[20] Note that in some cases, the torque from paramagnetic response can be ignored compared with the vortex torque, such as in MgB_2,[23] but in other cases, the paramagnetic torque is comparable with the vortex torque, such as in heavy fermion superconductor $CeCoIn_5$.[19] Our results show that $Ca_{0.73}La_{0.27}(Fe_{0.96}Co_{0.04})As_2$ belongs to the second case. In order to obtain the vortex torque in the mixed state, one needs to account for this paramagnetic contribution and subtract it from the measured torque.[16,19]

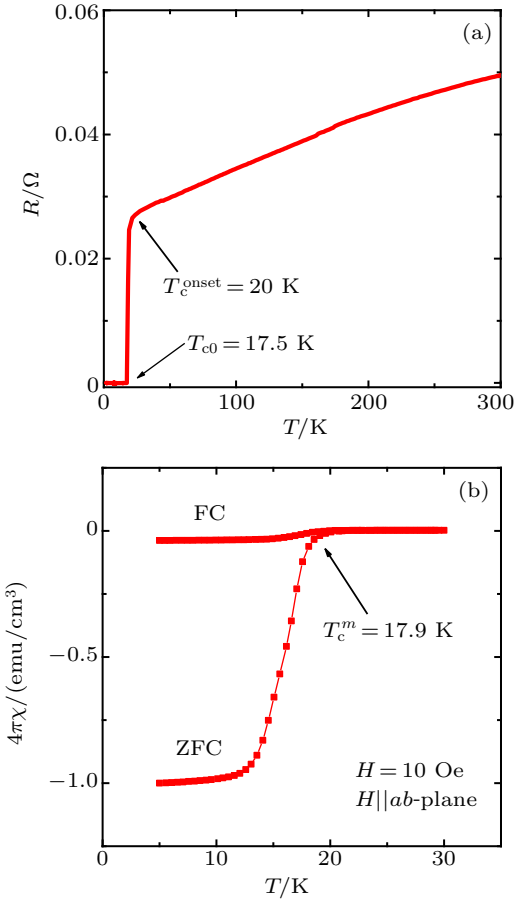

Fig. 1. (a) Temperature dependent R of $Ca_{0.73}La_{0.27}(Fe_{0.96}Co_{0.04})As_2$. (b) Temperature T dependent normalized magnetization data for $H = 10$ Oe under both zero-field-cooled (ZFC) and field cooled (FC) conditions.

The anisotropy parameter γ is an important quantity for characterizing superconductivity. Here we examine the anisotropy γ of $Ca_{0.73}La_{0.27}(Fe_{0.96}Co_{0.04})As_2$ by studying the torque data in the mixed state for $T < T_c$. Figure 3(a) shows the torque data measured at $T = 17$ K and $H = 3$ T, which is the typical behavior in the mixed state. With increasing and decreasing angular sweeps, a large hysteresis is observed,

which is a result of intrinsic pinning of vortices. The reversible part of the torque can be obtained by $\tau_{\rm rev} = (\tau_{\rm inc} + \tau_{\rm dec})/2$, where $\tau_{\rm inc}$ and $\tau_{\rm dec}$ indicate torque data measured with increasing and decreasing angle sweeps, respectively. Only $\tau_{\rm rev}$ reflects the equilibrium state which allows the determination of thermodynamic parameters. Figure 3(b) plots $\tau_{\rm rev}$ for the data measured at $T = 17$ K with different applied magnetic fields. The symbols are data points and the solid lines are fitting curves by the following equation:

$$\tau_{\rm rev}(\theta) = a\sin 2\theta + \frac{\varphi_0 HV}{16\pi\mu_0\lambda_{ab}^2}\frac{\gamma^2-1}{\gamma}\frac{\sin 2\theta}{\varepsilon(\theta)}\ln\left\{\frac{\gamma\eta H_{c2}^{\|c}}{H\varepsilon(\theta)}\right\}, \quad (5)$$

where a is a fitting parameter, φ_0 is the flux quantum, V is the volume of the sample, μ_0 is the vacuum permeability, λ_{ab} is the penetration depth in the ab-plane, γ is the anisotropy parameter, $\varepsilon(\theta) = \left(\sin^2\theta + \gamma^2\cos^2\theta\right)^{1/2}$, η is a numerical parameter of the order of unity, which accounts for the structure of the vortex core, and $H_{c2}^{\|c}$ is the upper critical field parallel to the c-axis. We define $\beta \equiv \varphi_0 HV/16\pi\mu_0\lambda_{ab}^2$. In the above equation, the torque data include two contributions. The first term is from paramagnetism and the second one is from the Abrikosov vortex which can be described by the Kogan's model.[15]

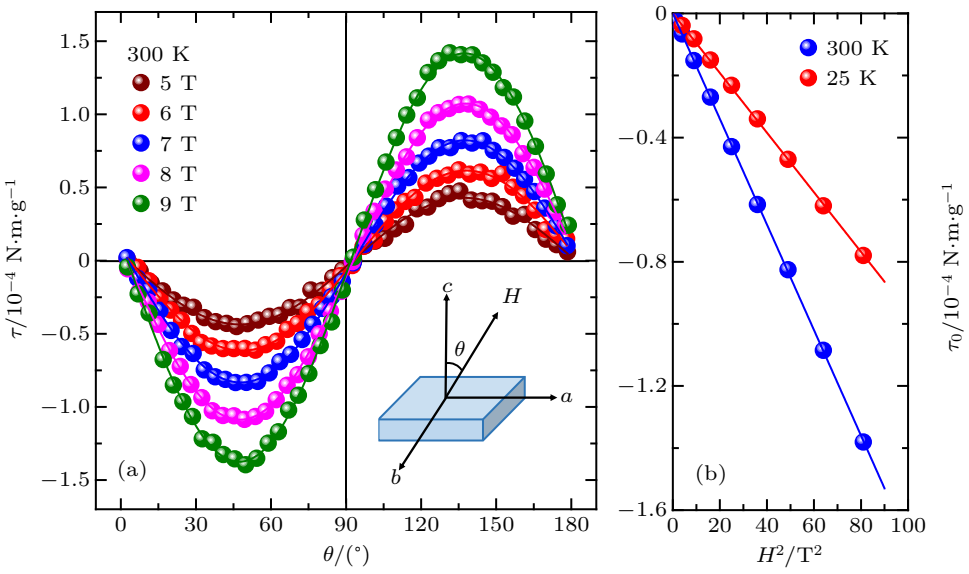

Fig. 2. (a) Typical angular θ dependent torque τ at $T = 300$ K with a magnetic field $H = 5$ T, 6 T, 7 T, 8 T, 9 T. The solid lines are fits of the data with $\tau = \tau_0 \sin 2\theta$. Inset: sketch of the single crystal with the orientation of the magnetic field H with respect to the crystallographic axes. (b) The torque coefficient τ_0 vs. H^2 at $T = 25$ K and 300 K. The solid lines are linear fit of the data.

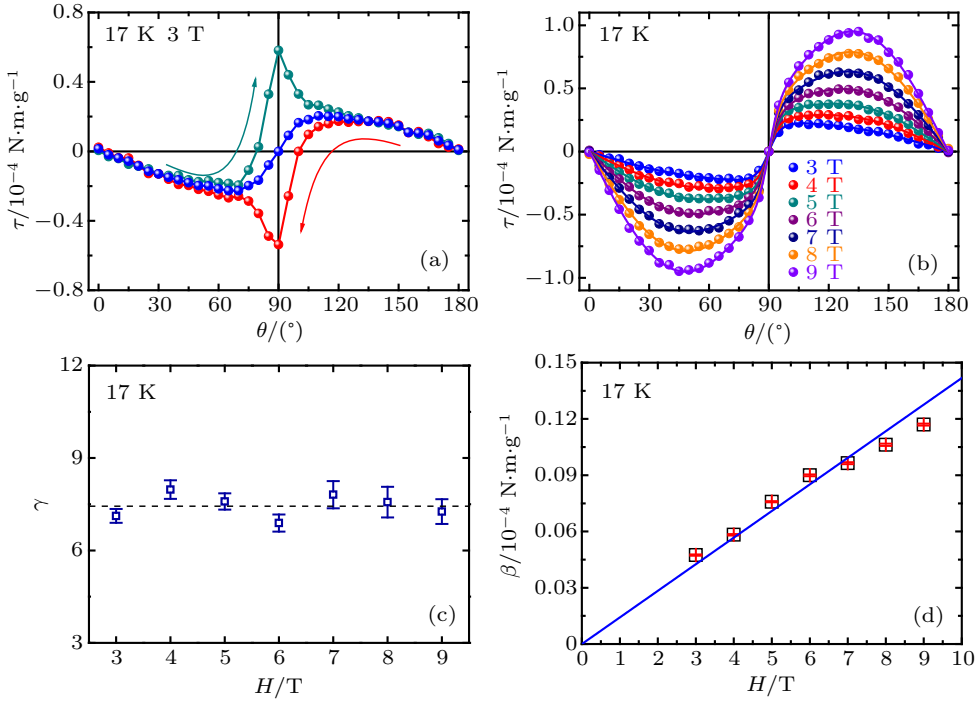

Fig. 3. (a) Angle θ dependence of the torque τ measured in increasing (green) and decreasing (red) angle at $T = 17$ K and $H = 3$ T, and the reversible torque $\tau_{\rm rev}$ (blue). (b) $\tau_{\rm rev}$ vs. θ for $H = 3$ T, 4 T, 5 T, 6 T, 7 T, 8 T, 9 T. The solid lines are fitting curves by Eq. (5). (c) The magnetic field H dependence of anisotropy parameter γ. (d) H dependence of the fitting parameter β. The solid line is a guide to the eyes.

The magnetic field dependence of the anisotropy parameter γ is summarized in Fig. 3(c). It is found that, γ exhibits weak magnetic field dependence. At the reduced temperature $t = 0.85$, $\gamma \simeq 7.5$. The anisotropy parameter γ of the 11 and 122 families of FeSCs stays in the range of 2–3,[24] like for $FeSe_{0.5}Te_{0.5}$, $\gamma \simeq 3.1$ at $t = 0.86$ determined by torque measurements.[27] For 1111 family of FeSCs, like $SmFeAsO_{0.8}F_{0.2}$, $\gamma \simeq 12$ at $t = 0.8$,[25] $CaFe_{0.88}Co_{0.12}AsF$ $\gamma \simeq 15$ at $t = 0.83$.[16] So, the sample examined in this work is more anisotropic compared to 11 and 122 families, but less anisotropic than 1111 families of FeSCs. Similar conclusion can be reached based on γ_H $(= H_{c2}^{||ab}/H_{c2}^{||c})$ of 11, 122, and 1111 families of FeSCs.[24,28] The relatively large anisotropy of CaLa112 may result from the large distance d (~ 1.035 nm) between the adjacent FeAs layers.[11] Note that this material crystallizes in a low symmetry crystal structure with an additional metallic spacer-layer which significantly increases the distance between the superconducting FeAs layers.[29] Figure 3(d) is a plot of the field dependence of β. Note that β displays linear behavior with zero y-intercept, as it should be, and based on which the penetration depth can be obtained.

Figure 4(a) plots τ_{rev} for the data measured with $H = 9$ T at different temperatures. Figure 4(b) summarizes the temperature T dependence of the anisotropy parameter γ. Note that with increasing temperature, γ decreases fast, at $t = 0.75$, $\gamma \simeq 11.45$, and at $t = 0.9$, $\gamma \simeq 6.84$. The fact that γ is not a constant suggests that $Ca_{0.73}La_{0.27}(Fe_{0.96}Co_{0.04})As_2$ is probably a multiband/multigap superconductor. This multiband picture is consistent with other reports. For example, Xing *et al.* reported that a two-band model is required to fully reproduce the behavior of $\mu_0 H_{c2}^{||c}(T)$ in $Ca_{0.8}La_{0.2}Fe_{0.98}Co_{0.02}As_2$, in which $\mu_0 H_{c2}^{||c}(T)$ presents a sublinear temperature dependence with decreasing temperature.[30] Note that multiband picture is also reported in other FeSCs, such as $LaFeAsO_{0.9}F_{0.1}$,[20] $SmFeAsO_{0.8}F_{0.2}$,[25] and $FeSe_{0.5}Te_{0.5}$.[27]

In Fig. 4(b), we also compare our data and other reports for similar compounds.[11,12,30] It is found that the Co-doped 112 system is more anisotropic than the one without doping at temperature close to T_c. Furthermore, it is found that for Co-doped 112 system, the anisotropy determined from our torque measurements γ_λ, and the one based on upper critical field γ_H, show opposite temperature dependence at low temperatures. Note that for a multiband superconductor at arbitrary temperatures, γ_H and γ_λ are not necessarily the same, since the former determines the anisotropy of the coherence length, while the latter describes the ellipticity of the current distribution far from the core.[31] However, the anisotropy parameters determined by different techniques tend to meet at T_c as shown in Fig. 4(b).

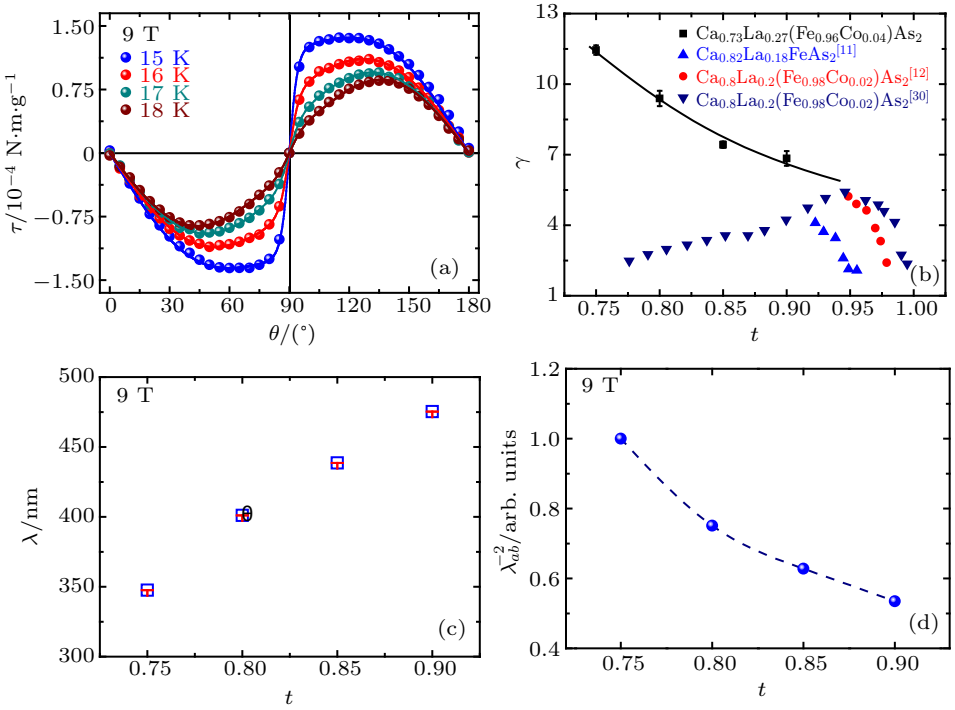

Fig. 4. (a) The reversible part of the torque data τ_{rev} for $T = 15$ K, 16 K, 17 K,18 K with $H = 9$ T. The solid lines are fitting curves by Eq. (5). (b) The reduced temperature t (T/T_c) dependence of the anisotropy parameter γ. The squares represent data obtained from our torque measurements. The blue triangles represent data of $Ca_{0.82}La_{0.18}FeAs_2$,[11] others symbols represent data for $Ca_{0.8}La_{0.2}(Fe_{0.98}Co_{0.02})As_2$[12] and $Ca_{0.8}La_{0.2}(Fe_{0.98}Co_{0.02})As_2$,[30] respectively. The solid line is a guide to the eyes. (c) The reduced temperature t dependence of the in-plane penetration depth λ_{ab}. (d) The reduced temperature t dependence of the superfluid density $n_s \propto \lambda^{-2}$ extracted from the torque data at $H = 9$ T. The dashed line is a guide to the eyes.

From Eq. (2), we can also obtain the temperature dependence of penetration depth λ_{ab}, as shown in Fig. 4(c). It is found that λ_{ab} increases with increasing temperature. At $t = 0.75$, $\lambda_{ab} = 347$ nm. At $t = 0.9$, $\lambda_{ab} = 475$ nm. This is consistent with an earlier report $\lambda_{ab}(0) = 300$–500 nm.[32] In addition, λ^{-2} shows a pronounced positive curvature (Fig. 4(d)), similar to that of MgB_2[33] and $LaFeAsO_{0.9}F_{0.1}$.[20] Such an upward curvature is consistent with the $s^{\pm}$ scenario with interband impurity scattering.[34]

4. Conclusion and perspectives

In summary, we performed detailed angular dependent torque measurements on $Ca_{0.73}La_{0.27}(Fe_{0.96}Co_{0.04})As_2$. A large paramagnetic effect is observed in the normal state. In the mixed state, we obtain the anisotropy parameter from the reversible torque. The moderate anisotropy shows that this 112 FeSC is more anisotropic in the mixed state compared to 11 and 122 families of FeSCs, but less anisotropic than 1111 families of FeSCs. We also investigate its temperature and magnetic field evolution. The fact that the anisotropy parameter is not a constant points to a possible multiband picture. At low temperatures, our anisotropy parameter shows different behavior from the one determined by transport measurements, similar to the iron-based superconductor $FeSe_{0.5}Te_{0.5}$, $Ba_{1-x}K_xFe_2As_2$[24] and the two-gap superconductor MgB_2.[23]

References

[1] Yang J, Zhou R, Wei L L, Yang H X, Li J Q, Zhao Z X and Zheng G Q 2015 *Chin. Phys. Lett.* **32** 107401

[2] Ren Z A, Lu W, Yang J, Yi W, Shen X L, Li Z C, Che G C, Dong X L, Sun L L, Zhou F and Zhao Z X 2008 *Chin. Phys. Lett.* **25** 2215

[3] Fujioka M, Denholme S J, Tanaka M, Hiroyuki Takeya, Takahide Y and Yoshihiko T 2014 *Appl. Phys. Lett.* **105** 102602

[4] Wang R, Li D P 2016 *Chin. Phys. B* **25** 097401

[5] Tapp J H, Tang Z, Lv B, Kalyan S, Bernd L, Chu C W and Guloy M 2008 *Phys. Rev. B* **78** 060505

[6] Zhu J, Wang Z S, Wang Z Y, Hou X Y, Luo H Q, Lu X Y, Li C H, Shan L, Wen H H, Ren C 2015 *Chin. Phys. Lett.* **32** 77401

[7] Kawasaki S, Mabuchi T, Maeda S, Tomoki Adachi, Mizukami T, Kudo K, Nohara M and Zheng G Q 2015 *Phys. Rev. B* **92** 180508

[8] Xie T, Gong D L, Zhang W L, Gu Y H, Hüsges Z, Chen D F, Liu Y T, Hao L J, Meng S Q, Lu Z L, Li S L and Luo H Q 2017 *Supercond. Sci. Technol.* **30** 095002

[9] Zhou W, Ke F, Xu X, Sankar, Xing X, Xu C Q, Jiang X F, Qian B, Zhou N, Zhang Y, Xu M, Li B, Chen Band Shi Z X 2017 *Phys. Rev. B* **96** 184503

[10] Xing X Z, Li Z F, Veshchunov I, Yi X L, Meng Y, Li M, Lin B C, Tamegai T and Shi Z X 2019 *New J. Phys.* **21** 093015

[11] Zhou W, Zhuang J, Yuan F, Li X, Xing X Z, Sun Y and Shi Z X 2014 *Appl. Phys. Express* **7** 063102

[12] Xing X, Zhou W, Zhou N, Yuan F F, Pan Y Q, Zhao H J, Xu X F and Shi Z X 2016 *Supercond. Sci. Tech.* **29** 055005

[13] Takahashi K, Atsumi T, Yamamoto N, Xu M X, Hideaki K and Takekazu I 2002 *Phys. Rev. B* **66** 012501

[14] Kortyka A, Puzniak R Wisniewski A, Zehetmayer M, Weber H W, Cai Y Q and Yao X 2010 *Supercond. Sci. Tech.* **23** 065001

[15] Kogan V G 1988 *Phys. Rev. B* **38** 7049

[16] Xiao H, Gao B, Ma Y H, Li X J, Mu G and Hu T 2016 *J. Phys.: Condens. Matter* **28** 325701

[17] Yu A B, Wang T Wu Y F, Huang Z, Xiao H, Mu G and Hu T 2019 *Phys. Rev. B* **100** 144505

[18] Xiao H, Hu T, Zhou H J, Li X J, Ni S L, Zhou F and Dong X L 2020 *Phys. Rev. B* **101** 184520

[19] Xiao H, Hu T, Almasan C C, Sayles T A and Maple M B 2006 *Phys. Rev. B* **73** 184511

[20] Li G, Grissonnanche G, Gurevich A, Zhigadlo N D, Katrych S, Bukowski Z, Karpinski J and Balicas L 2011 *Phys. Rev. B* **83** 214505

[21] Kasahara S, Shi H J, Hashimoto K, Tonegawa S, Mizukami Y, Shibauchi T, Sugimoto K, Fukuda T, Terashima T, Nevidomskyy A H and Matsuda Y 2012 *Nature* **486** 382

[22] Bergemann C, Tyler A W, Mackenzie A P, Cooper J R, Julian S R and Farrell D E 1998 *Phys. Rev. B* **57** 14387

[23] Angst M, Puzniak R, Wisniewski A, Jun J, Kazakov S M, Karpinski J, Roos J and Keller H 2002 *Phys. Rev. Lett.* **88** 167004

[24] Khasanov R and Guguchia Z 2015 *Supercond. Sci. Tech.* **28** 034003

[25] Weyeneth S, Puzniak R, Mosele U, Zhigadlo N D, Katrych S, Bukowski Z, Karpinski J, Kohout S, Roos J and Keller H 2009 *J. Supercond. Nov. Magn.* **22** 325

[26] Jiang, S, Liu, L, Schütt, M, Hallas, Hallas M, Shen B, Tian W, Emmanouilidou E, Shi A S, Luke M, Yasutomo J U, Fernandes R M and Ni N 2016 *Phys. Rev. B* **93** 174513

[27] Bendele M, Weyeneth S, Puzniak R, Maisuradze A, Pomjakushina E, Conder K, Pomjakushin V, Luetkens H, Katrych S, Wisniewski A, Khasanov R and Keller H 2010 *Phys. Rev. B* **81** 224520

[28] Zhou W, Xing X Z, Wu W J, Zhao H J and Shi Z X 2016 *Sci. Rep.* **6** 22278

[29] Prozorov R, Ni N, Tanatar M A, Kogan V G, Gordon R T, Martin C, Blomberg E C, Prommapan P, Yan J Q, Budko S L and Canfield P C 2008 *Phys. Rev. B* **78** 224506

[30] Xing X, Zhou W, Wang J, Feng J J, Xu C Q, Zhou N, Meng Y, Zhang Y F, Pan Y Q, Qin L Y, Zhou W, Zhao H J and X1 Z 2017 *Sci. Rep.* **7** 45943

[31] Xiao H, Hu T, Almasan C C, Sayles T A and Maple M B 2008 *Phys. Rev. B* **78** 014510

[32] Xing X Z, Li Z F, Yi X L, *et al.* 2018 *Sci. Chin. Phys. Mech. Astron.* **61** 127406

[33] Fletcher J D, Carrington A, Taylor O J, Kazakov S M and Karpinski J 2005 *Phys. Rev. Lett.* **95** 097005

[34] Martin C, Tillman M E, Kim H, Roos J, Keller H, Miranovic P, Jun J, Kazakov S M and Karpinski J 2009 *Phys. Rev. Lett.* **102** 247002